

See discussions, stats, and author profiles for this publication at: <https://www.researchgate.net/publication/7626111>

Modifications to the Tetracaine Scaffold Produce Cyclic Nucleotide-Gated Channel Blockers with Widely Varying Efficacies

ARTICLE *in* JOURNAL OF MEDICINAL CHEMISTRY · OCTOBER 2005

Impact Factor: 5.45 · DOI: 10.1021/jm0502485 · Source: PubMed

CITATIONS

8

READS

24

9 AUTHORS, INCLUDING:



Ambarish S Ghatpande

Indian Institute of Science

11 PUBLICATIONS 152 CITATIONS

SEE PROFILE



Tapasree Banerji

Oregon Health and Science University

9 PUBLICATIONS 141 CITATIONS

SEE PROFILE



Patrick G. McDougal

Reed College

24 PUBLICATIONS 1,177 CITATIONS

SEE PROFILE



Jeffrey W Karpen

Touro University College of Osteopathic Medi...

58 PUBLICATIONS 2,529 CITATIONS

SEE PROFILE

Published in final edited form as:

J Med Chem. 2005 September 8; 48(18): 5805–5812.

Modifications to the Tetracaine Scaffold Produce Cyclic Nucleotide-Gated Channel Blockers with Widely Varying Efficacies

Timothy Strassmaier[†], Ramalinga Uma[†], Ambarish S. Ghatpande[‡], Tapasree Bandyopadhyay[†], Michelle Schaffer[§], John Witte[§], Patrick G. McDougal[§], R. Lane Brown^{||}, and Jeffrey W. Karpen^{*,†}

[†]Department of Physiology and Pharmacology, Oregon Health & Science University, Portland, Oregon 97239

[‡]Department of Physiology and Biophysics, University of Colorado Health Sciences Center, Denver, Colorado 80262

[§]Department of Chemistry, Reed College, Portland, Oregon 97202

^{||}Neurological Sciences Institute, Oregon Health & Science University, Portland, Oregon 97239

Abstract

Five new tetracaine analogues were synthesized and evaluated for potency of blockade of cyclic nucleotide-gated channels relative to a multiply charged tetracaine analogue described previously (4). Increased positive charge at the tertiary amine end of tetracaine results in higher potency and voltage dependence of block. Modifications that reduce the hydrophobic character at the butyl tail are deleterious to block. The tetracaine analogues described here have apparent affinities for CNGA1 channels that vary over nearly 8 orders of magnitude.

Introduction

In photoreceptor cells of the retina and sensory neurons of the olfactory epithelium, cyclic nucleotide-gated (CNG) channels play a key role in the signal transduction cascade, translating a change in cyclic nucleotide concentration into an electrical response.^{1,2} While CNG channels are only weakly voltage-dependent, they bear significant similarity to voltage-dependent potassium channels in their architecture.^{3,4} They share a common topology of six transmembrane helices (S1–S6) per subunit and assemble into functional tetramers, with the pore region formed by the S5/S6 loop.^{5–11} Despite their limited voltage dependence, CNG channels contain a vestigial “voltage sensor” in S4. CNG channels are distinguished by the presence of a cyclic nucleotide-binding domain on the cytoplasmic face of the channel downstream from S6. Channel activation is dependent upon cyclic nucleotide concentration; binding of three cyclic nucleotides per tetramer causes significant channel opening, while full activation requires four.^{12–14}

* Corresponding author: Department of Physiology and Pharmacology, Oregon Health & Science University, 3181 SW Sam Jackson Park Rd., Portland, OR 97239. Phone 503-494-7463; e-mail karpenj@ohsu.edu.

Supporting Information Available: HPLC analyses for compounds 2, 3, 14, and 15 and combustion analyses for compounds 14 and 16. This information is available free of charge via the Internet at <http://pubs.acs.org>.

Although CNG channels are expressed in other sensory and nonsensory tissues, their physiological roles are unclear beyond the well-characterized visual and olfactory systems.¹⁵ Efforts to elucidate the role of CNG channels are hampered by the lack of highly selective pharmacological agents. Several compounds are demonstrated blockers of CNG channels, including *l*-cis-diltiazem and the tertiary amine local anesthetic tetracaine [2-(dimethylamino) ethyl 4-(butylamino)benzoate] (**1**).^{16,17} These agents are nonideal due to their relatively low efficacy (apparent affinities in the micromolar range) and their lack of selectivity. In one regard, however, this promiscuity has been useful; analysis of the interaction between sodium channels and local anesthetics and anti-arrhythmics can provide useful insights into block of CNG channels. Mutagenesis studies of sodium channels suggest a bimodal interaction: electrostatic interactions with residues in the selectivity filter and hydrophobic interactions with aromatic residues on the putative pore-forming helix.¹⁸⁻²¹ Similar mutagenesis studies have demonstrated that these electrostatic interactions are conserved in the interaction between tetracaine and CNG channels.²² It has become apparent that the mechanisms of local anesthetic block of sodium and CNG channels are not identical. In sodium channels, it has been demonstrated that local anesthetics have greater affinity for the channel in its open and inactivated states, a phenomenon referred to as “use-dependent” blockade. However, tetracaine binds preferentially to the closed state of CNG channels.¹⁷

The goal of this study was to synthesize and examine a series of tetracaine analogues, in an attempt to determine the effects of modifications at different positions on the tetracaine core for block of homotetrameric CNG channels. We used the retinal rod channel α subunit, CNGA1, in these studies. We have reported previously that a multiply charged analogue of tetracaine, compound **4**, blocks CNGA1 channels at subnanomolar concentrations.²³ Furthermore, we demonstrated that this compound was selective for CNG channels relative to sodium channels. We hypothesize that the high affinity and selectivity results from the targeting of the multiple positive charges to the high negative charge density of the CNG channel selectivity filter.^{24,25} The majority of CNG channels are thought to have a net charge of -3 in the selectivity filter,²⁶⁻²⁸ whereas the sodium channel selectivity filter is predicted to have a net -1 charge.²⁹ We describe here a series of tetracaine analogues with variations in the number and position of positive charges and/or modifications of the hydrophobic alkyl chain. Successive addition of positive charge to the tertiary amine (**3**, **4**) results in dramatic increases in potency. The profound reduction in efficacy due to removal or modification of the butyl tail (**14**, **15**, **16**) confirms the importance of hydrophobic interactions. Our results provide direction for the development of more potent and selective CNG channel antagonists based on the tetracaine scaffold.

Chemistry

Synthesis of tetracaine derivatives with one (**3**) or two (**4**) propylamino groups attached in tandem to the tertiary amine was achieved by reaction of tetracaine with 3-bromopropylamine followed by separation of **3** and **4** by silica gel chromatography and high-performance liquid chromatography (HPLC). A similar reaction of tetracaine with 1-bromobutane yielded a tetracaine analogue with a permanent positive charge and increased nonpolar bulk (**2**) (Scheme 1). Derivatization of the butyl chain of tetracaine (**1**) required rebuilding the tetracaine core starting with an appropriately functionalized 4-carbon chain (**5**) (Scheme 2). This strategy resulted in the production of a tetracaine analogue with a primary amine appended at the end of the butyl tail (**14**) in eight steps. The *N*-acetyl-modified tetracaine analogue (**15**) was synthesized in one additional step. Finally, a tetracaine analogue lacking a butyl group (**16**) was synthesized in two steps starting from 4-nitrobenzoyl chloride.

Results

We synthesized five analogues of tetracaine to introduce modifications at either end of the molecule, specifically at the hydrophobic butyl group or the positively charged tertiary amine (Schemes 1 and 2). To assess the relative potency and voltage dependence of block of each analogue, we expressed homomeric CNGA1 channels in *Xenopus laevis* oocytes and recorded currents through these channels in excised inside-out patches. Compounds were applied to the bath in the presence of a saturating concentration of cGMP. In the absence of blockers, each voltage step was accompanied by a characteristic decay of current from a peak value immediately following the voltage change (Figure 1). This current “droop” results from a change in chemical driving force due to hindered diffusion of ions at the surface of the excised patch and varies with the square of the current.³⁰ For calculating fractional block, steady-state currents measured at the end of a voltage pulse have been corrected for the effects of ion accumulation/depletion as described in the Experimental Section.

We previously reported a multiply charged, extremely potent CNG channel blocker, compound **4**, which features the addition of two propylamino groups to tetracaine's tertiary amine.²³ We isolated a related derivative (**3**) with a single added propylamino group. Under physiological conditions **1**, **3**, and **4** will bear one, two, and three positive charges, respectively. The addition of positive charge to the tertiary amine of tetracaine gave rise to a dramatic increase in apparent affinity for the channel at +40 mV. We determined that **3** and **4** were approximately 2 and 5 orders of magnitude more potent than tetracaine, respectively (Figure 1, Table 1). The importance of additional positive charge is underscored by the observation that **2**, which is isosteric with **3** but carries only a single charge, was only a marginally more effective blocker than tetracaine (Figure 1, Table 1).

We also assessed the impact of modification of the tetracaine scaffold at the opposite end, by altering the butyl tail. A tetracaine analogue that lacks the butyl tail entirely (**16**) had an apparent affinity for CNGA1 channels more than 300-fold lower than that of tetracaine. Likewise, two tetracaine analogues modified at the butyl tail with a positively charged amine (**14**) or a polar *N*-acetyl group (**15**) were approximately 30- and 350-fold less potent than tetracaine at +40 mV (Figure 1, Table 1).

An inspection of the raw current traces in Figure 1 gives an indication of the voltage dependence of block. Each of the analogues was a more effective antagonist at positive potentials, with a larger fraction of the control current blocked at +40 mV than at -80 mV. Relief of block was observed as an increase in the inward current following repolarization to -80 mV from +40 mV. For each analogue, we examined the fraction of current blocked over a range of potentials and fit these data with the Woodhull model for voltage-dependent block.³¹ From these data we determined the apparent affinity of each analogue at 0 mV ($K_{D(0)}$) and the $z\delta$ value, which in the simplest model is equivalent to the charge carried by a blocker (z) multiplied by the fraction of the electric field (δ) traversed to reach its binding site (Figure 2, Table 1).

For most of the analogues, derivatization of tetracaine (**1**) had predictable effects on the $z\delta$ value. Successive addition of positive charge to the tertiary amine resulted in increased $z\delta$ values. Tetracaine had a $z\delta$ value of 0.47; addition of one positively charged propylamino group (**3**) increased the $z\delta$ to 1.8, and with two additional charges (**4**) the $z\delta$ was 2.6. As expected, the addition of a nonpolar butyl group to tetracaine's tertiary amine (**2**) had no appreciable impact on voltage dependence of block. Likewise **15**, with a polar but uncharged modification to the butyl chain, had a $z\delta$ value of 0.47. Interestingly, **16**, which lacks the butyl chain, displayed a steeper voltage dependence of block with a $z\delta$ of 0.9. Finally, we observed that addition of a positive charge to the butyl chain (**14**) yielded a much smaller increase in voltage dependence ($z\delta = 1.1$) than measured for compound **3**, with an additional positive charge at

the tertiary amine (Figure 2, Table 1). Analysis of the $K_{D(0)}$ values, a measurement of the inherent affinity of the blocker for the channel, reveals that the order of potency of the compounds is unchanged relative to the apparent affinities measured at +40 mV (Table 1).

Significant current droop due to the ion accumulation/ depletion in most patches made a careful analysis of the kinetics of block difficult. However, we did notice that in most cases block by tetracaine analogues with modifications of the butyl tail, compounds **14**, **15**, and **18**, demonstrated a slow kinetic component (Figures 1 and 2). Double-exponential fits of the data suggested a minor contribution to overall block (not shown). Qualitatively, the kinetics of block by compound **14** were noticeably different from the other analogues (Figure 2). In particular, relief of block at -80 mV was greatly slowed. We also observed biphasic kinetics upon steps to depolarized potentials, with a large fraction of block occurring too quickly to be resolved, followed by a significantly slower phase.

Discussion

We have synthesized five new analogues of tetracaine that, together with the previously reported compound **4**, vary over nearly 8 orders of magnitude in their apparent affinity for CNGA1 channels at positive potentials. Given the limited number of compounds examined, the large range of apparent affinity is striking. Some of the increase in potency for the multiply charged analogues, **3** and **4**, at +40 mV is clearly due to increased voltage dependence of block. It is worth noting that each addition of a charged propylamino group is associated with an increase of $\sim 1 z\delta$. Given that polyamines are permeant blockers of CNG channels, it is possible that the tetracaine core docks in the channel such that its amine group contacts the negatively charged pore glutamates,²² with additional propylamino groups threading further into the pore, perhaps reaching beyond the selectivity filter.³² On the other hand, the $K_{D(0)}$ values derived from fits to the Woodhull model show that the increased apparent affinity measured at +40 mV is not solely due to the electric field but also reflects a greater interaction with the channel pore. The addition of a single propylamino group (**3**) reduces the $K_{D(0)}$ by an order of magnitude; further addition of a second propylamino (**4**) group reduces the $K_{D(0)}$ by more than 3 orders of magnitude with respect to **1**. The larger jump in affinity associated with the addition of a second propylamino group is striking. One possibility is that the tertiary amine of tetracaine may not be in direct contact with the pore glutamates in the most stable bound configuration, while the terminal amine of **4** gets much closer. Alternatively, if the added propylamino groups of **4** penetrate the pore, as discussed above, the terminal amine may encounter favorable electrostatic interactions beyond the selectivity filter, to explain the increase in intrinsic affinity. In either case, varying the linker between amines (e.g., ethyl vs propyl) could provide a better fit with the channel and an even more potent derivative.

While appending a primary amino group to the hydrophobic end of tetracaine (**14**) significantly decreases the apparent affinity for CNGA1 channels, the charged group does appear to contribute to the voltage dependence of block. The $z\delta$ value for **14** is increased relative to tetracaine (**1**) (1.1 versus 0.47). The simplest explanation is that the introduction of positive charge interferes with the hydrophobic interaction but contributes to block at positive potentials by traversing a portion of the electric field. When the primary amine of **14** is acetylated to yield **15**, neutralizing the positive charge, the intrinsic interaction with the channel decreases in affinity by ~ 4 -fold. Taken together, these results indicate that any polar bulk at the end of the butyl tail is poorly tolerated. Given that block of CNGA1 channels is sensitive to addition of polar groups to tetracaine's hydrophobic end, it is not surprising that removal of the butyl chain (**16**) is deleterious. Interestingly, the $z\delta$ value for this compound is significantly higher than that found for tetracaine (**1**), 0.91 and 0.47, respectively. The simplest reasoning would be that the tertiary amine of **16** penetrates further into the pore on average, perhaps due to the loss of the hydrophobic interaction. However, the observation that **15** has a similarly weak interaction

with the channel but no obvious change in voltage dependence could call this explanation into question. At physiological pH the aromatic amine of **16** is expected to be uncharged. However, it is possible that in the context of the channel pore the pK_a of this group ($pK_a = 4-5$) could be perturbed, resulting in the aromatic amine carrying some positive charge. It should be noted that tetracaine (**1**) and compound **4** have been shown to be state-dependent blockers of CNG channels, strongly preferring closed over open channels.^{17,22,23} We have not investigated this issue with the new derivatives. Some of the observed differences between blockers could arise from disparities in the state dependence of block. It is also known that the simple Woodhull model does not account for all of the complexities of voltage-dependent block.

These results will guide future modifications of tetracaine toward the goal of synthesizing a blocker selective for CNG channels. As previously reported, the high affinity of **4** for CNGB1 channels at positive potentials is accompanied by a significant increase in the selectivity for CNGB1 channels relative to voltage-gated sodium channels. We will alter this scaffold in an attempt to further enhance selectivity, by varying the distance between the positive charges. We are also interested in generating a series of derivatives with nonpolar substitutions (e.g., shorter, longer, branched, or aromatic groups) of the butyl tail to target unique features of the CNG channel pore. We anticipate that a higher affinity compound would also show increased block at physiological potentials. We may also achieve selectivity through the synthesis of bivalent compounds that link the tetracaine blocker with the cGMP agonist moiety.³³ Our results here indicate that the amine end of **3** or **4** is a prime target for attachment of a flexible polymer derivatized with cGMP. Such bivalent compounds hold promise as highly potent and selective inhibitors of CNG channels.

Experimental Section

Channel Expression and Electrophysiology

Bovine CNGB1 cDNA in the plasmid, pGEM-HE, was linearized with *NheI* and used as a template for production of CNGB1 cRNA by use of the mMESSAGE mMACHINE kit (Ambion, Austin, TX). *Xenopus* oocytes were microinjected with 5–25 ng of cRNA and incubated at 18 °C. Inside-out excised patch recordings were made 1–6 days after injection, at room temperature with an Axopatch 200A amplifier (Axon Instruments, Foster City, CA). Electrodes pulled from borosilicate glass and heat-polished had resistances between 0.7 and 2.1 MΩ. Pipet and bath solutions were identical and consisted of 130 mM NaCl, 2 mM *N*-(2-hydroxyethyl)piperazine-*N'*-2-ethanesulfonic acid (HEPES), 1 mM ethylene glycol bis(β -aminoethyl ether)-*N,N,N',N'*-tetraacetic acid (EGTA), and 0.02 mM ethylenediaminetetraacetic acid (EDTA), pH 7.6. Currents were low-pass-filtered with an eight-pole Bessel filter and sampled at 4–5 times the filter frequency. For shorter depolarizations (10 s duration) the sampling rate was 4 kHz, while longer pulses (40 s duration) were sampled at 1 kHz. For analysis, currents in the absence of cGMP were subtracted from all traces. For patches with high current density, currents were corrected for series resistance errors. To correct steady-state currents for the droop associated with ion accumulation/depletion, the following equation was used: $I_{\text{corr}} = [(g_v/g_0)(I_v/|I_{-80}|)(\Delta I_{-80})] + I_v$, where g_v and g_0 are the slope conductances at a test potential and 0 mV, respectively, I_v is the steady-state current at a test potential, $|I_{-80}|$ is the absolute value of the steady-state current at –80 mV, and ΔI_{-80} is the peak rebound current after a voltage step from –80 to 0 mV.

Chemistry

All reagents were obtained from Sigma-Aldrich and solvents from Fisher. Reactions were followed by thin-layer chromatography (TLC) and visualized by UV shadowing. Ion-exchange HPLC was performed on a PolyCAT A, 21 × 250 mm, 5 μ m, 300 Å column (PolyLC, Southborough, MA) with a 5–500 mM ammonium acetate gradient (pH 5 with acetic acid).

Reversed-phase (RP) HPLC was performed on an Xterra Prep RP8, 19 × 100 mm, 5 μm column (Waters, Milford, MA) with a water–methanol gradient (5 mM ammonium acetate, pH 5).

***N*-(2-([4-(Butylamino)benzoyl]oxy)ethyl)-*N,N*-dimethylbutan-1-aminium Acetate (2)**

A mixture of tetracaine (**1**) (0.5 g, 1.89 mmol) and 1-bromobutane (215 μL, 2 mmol) in 10 mL of ethanol was refluxed for 72 h. Reaction progress was followed by TLC. Removal of solvent in vacuo gave a residue that was purified on a silica gel column; 175 mg (35%) of starting material and 145 mg (45%) of **2** were sequentially eluted with 2-propanol/acetic acid/water (5:3:2). ¹H NMR (400 MHz, CD₃OD) δ 7.78 (d, *J* = 9 Hz, 2H), 6.59 (d, *J* = 9 Hz, 2H), 4.91 (s, 1H, NH), 4.70 (br s, 2H), 3.78–3.80 (m, 2H), 3.41–3.44 (m, 2H), 3.20 (s, 6H), 3.14 (t, *J* = 7 Hz, 2H), 1.91 (s, 3H, CH₃COO[−]), 1.75–1.81 (m, 2H), 1.58–1.64 (m, 2H), 1.34–1.47 (m, 4H), 0.98 (t, *J* = 7.5 Hz, 3H), 0.97 (t, *J* = 7.5 Hz, 3H) (peak assignments were aided by ¹H–¹H COSY experiment); ¹³C NMR (125 MHz, CD₃OD) δ 179.4 (CH₃COO[−]), 167.7, 155.4, 132.9, 116.3, 112.3, 66.5, 64.1, 58.5, 52.2, 43.7, 32.4, 25.7, 23.8 (CH₃COO[−]), 21.4, 20.9, 14.4, 14.0; MS (ESI) *m/z* 321.3 (M)⁺.

3-Amino-*N*-(2-([4-(butylamino)benzoyl]oxy)ethyl)-*N,N*-dimethylpropan-1-aminium Acetate (3)

A mixture of tetracaine (**1**) (2.5 g, 9.46 mmol) and 3-bromopropylamine hydrochloride (2.1 g, 10 mmol) in 20 mL of ethanol was refluxed for 8 h. Reaction progress was followed by TLC. Removal of solvent in vacuo gave a residue that was purified by ion-exchange HPLC. Unreacted tetracaine (**1**) eluted first, compound **3** eluted second, followed by **4** in the ratio 67:27:6 (peak areas monitored at 312 nm). Compound **3** was further purified by RP-HPLC and dried repeatedly in a Speed-Vac (Savant). ¹H NMR (500 MHz, CD₃OD) δ 7.79 (d, *J* = 9 Hz, 2H), 6.60 (d, *J* = 9 Hz, 2H), 4.94 (s, 3H, NH), 4.73 (br s, 2H), 3.83–3.85 (m, 2H), 3.55–3.58 (m, 2H), 3.25 (s, 6H), 3.15 (t, *J* = 7 Hz, 2H), 2.96 (t, *J* = 7 Hz, 2H), 2.15–2.21 (m, 2H), 1.91 (s, 3H, CH₃COO[−]), 1.58–1.65 (m, 2H), 1.41–1.48 (m, 2H), 0.98 (t, *J* = 7 Hz, 3H) (peak assignments were aided by ¹H–¹H COSY experiment); ¹³C NMR (125 MHz, CD₃OD) δ 179.4 (CH₃COO[−]), 167.7, 155.42, 132.9, 116.3, 112.3, 64.7, 63.7, 58.5, 52.3, 43.8, 37.9, 32.4, 24.1 (CH₃COO[−]), 23.1, 21.4, 14.4; MALDI-MS (α-cyano-4-hydroxycinnamic acid matrix) *m/z* 322.23 (M)⁺.

3-[(3-Aminopropyl)amino]-*N*-(2-([4-(butylamino)-benzoyl]oxy)ethyl)-*N,N*-dimethylpropan-1-aminium Acetate (4)

See ref ²³ for this procedure.

***N*-(4-Bromophenyl)succinamide (7)**

To a solution of succinamic acid (**5**) (18.05 g, 0.154 mol) in dry DMF (130 mL) was added *N,N'*-carbonyldiimidazole (25 g, 0.154 mol) with stirring at room temperature under N₂. After evolution of CO₂ was complete (2 h), *p*-bromoaniline (**6**) (26.4 g, 0.154 mol) was added and the reaction proceeded for an additional 24 h. The mixture was concentrated in vacuo to a brown solid and washed with H₂O followed by CCl₄. Recrystallization from EtOAc and EtOH yielded a white crystalline product (**7**) (25 g, 60% yield). ¹H NMR (300 MHz, DMSO-*d*₆) δ 10.1 (s, 1H), 7.6 (d, *J* = 9 Hz, 2H), 7.4 (d, *J* = 9 Hz, 2H), 7.3 (s, 1H), 6.7 (s, 1H), 2.5 (t, *J* = 6.5 Hz, 2H), 2.37 (t, *J* = 6.4 Hz, 2H); ¹³C NMR (75 MHz, DMSO-*d*₆) δ 173.3, 170.8, 138.7, 131.4, 120.8, 114.3, 31.5, 29.8; GC–MS *m/z* 271 (M)⁺.

***N*-(4-Bromophenyl)butane-1,4-diamine (8)**

Borane dimethyl sulfide (26 g, 0.342 mol) was added dropwise over 0.5 h at 0 °C to a three-neck 250 mL round-bottom flask charged with **7** (23.4 g, 0.086 mol) in dry tetrahydrofuran (THF) and equipped with a pressure-equalizing addition funnel, thermometer, and reflux

condenser. The mixture was refluxed at 45 °C for 3 h and cooled to 25 °C, and MeOH (41 mL) was added dropwise. After the mixture was cooled to 5–10 °C, anhydrous HCl was bubbled in until pH 1.5–2.0 was reached. The resulting slurry was refluxed with the addition of MeOH (2 × 75 mL) until the precipitate had dissolved. The solvent was removed in vacuo; the resulting white solid was dissolved in H₂O (200 mL), and NaOH (~3.5 g) was added until pH 11.5 was reached. The mixture was extracted with CH₂Cl₂, dried (Na₂SO₄), evaporated in vacuo, and 18 g (58% yield) of **8** was purified on a silica gel column (CH₃CN/H₂O/AcOH 80:16:5). ¹H NMR (300 MHz, CDCl₃) δ 8.0 (s, 1H), 7.21 (d, *J* = 9 Hz, 2H), 6.45 (d, *J* = 9 Hz, 2H), 3.25 (t, *J* = 6.5 Hz, 2H), 2.85 (t, *J* = 6.4 Hz, 2H), 1.95 (s, 3H), 1.75 (m, 2H), 1.6 (m, 2H); ¹³C NMR (75 MHz, CDCl₃) δ 177.8, 147.2, 131.8, 114.2, 108.6, 43.0, 39.2, 26.0, 25.3, 23.1; GC–MS *m/z* 243 (MH)⁺.

***N*-[4-(Acetylamino)butyl]-*N*-(4-bromophenyl)acetamide (9)**

Et₃N (16.2 g, 0.16 mol) and acetic anhydride (14.2 g, 0.139 mol) were added to a solution of **8** (14.4 g, 0.04 mol) in CH₂Cl₂ (200 mL) with stirring under N₂. After 8 h the reaction was quenched with 1 N NaOH (200 mL) and extracted with CH₂Cl₂ (3 × 100 mL). The solvent was evaporated in vacuo, yielding a viscous yellow oil that was purified on a silica gel column eluted with CH₃CN/H₂O/AcOH (80:5:15). Final yield was 13.07 g (99%) of **9**. ¹H NMR (300 MHz, CDCl₃) δ 7.55 (d, *J* = 9 Hz, 2H), 7.05 (d, *J* = 9 Hz, 2H), 6.26 (s, 1H), 3.67 (t, *J* = 6.6 Hz, 2H), 3.23 (br q, 2H), 1.98 (s, 3H), 1.86 (s, 3H), 1.55 (m, 4H); ¹³C NMR (75 MHz, CDCl₃) δ 170.1, 141.8, 132.9, 129.6, 121.7, 48.4, 39.1, 26.1, 25.1, 23.1, 22.7; GC–MS *m/z* 327 (MH)⁺.

***N*-[4-(Acetylamino)butyl]-*N*-(4-cyanophenyl)acetamide (10)**

A solution of **9** (12.2 g, 0.037 mol) and CuCN (4.12 g, 0.046 mol) in dry *N*-methylpyrrolidinane (50 mL) was heated to 200 °C for 1.5 h. The reaction was quenched at room temperature with concentrated NH₃ (120 mL) and extracted with CH₂Cl₂ (3 × 100 mL). The combined extracts were dried (Na₂SO₄) and evaporated in vacuo to give a dark brown oil, which was purified on a silica gel column. Elution with EtOAc/isopropyl alcohol (IPA) (9:1) yielded 9.0 g (89% yield) of **10** as a pale yellow oil. ¹H NMR (300 MHz, CDCl₃) δ 7.76 (d, *J* = 9 Hz, 2H), 7.35 (d, *J* = 9 Hz, 2H), 6.17 (s, 1H), 3.75 (br t, 2H), 3.23 (br q, 2H), 1.98 (s, 3H), 1.90 (s, 3H), 1.55 (m, 4H); ¹³C NMR (75 MHz, CDCl₃) δ 170.1, 169.6, 146.8, 133.7, 128.7, 111.7, 48.7, 39.0, 26.2, 25.2, 23.1, 22.7; GC–MS *m/z* 274 (MH)⁺.

4-[(4-Aminobutyl)amino]benzoic Acid (11)

A solution of **10** (7.0 g, 0.026 mol) in HBr (80 mL) was heated under reflux for 4 h. HBr was removed in vacuo, and silica gel and H₂O were added. Volatiles were removed in vacuo and the silica gel mixture was applied to the top of a silica gel column and eluted with CH₃CN/H₂O/NH₃ (60:40:10) to give pure **11** (4.9 g, 85% yield). ¹H NMR (300 MHz, D₂O) δ 7.39 (d, *J* = 9 Hz, 2H), 6.42 (d, *J* = 9 Hz, 2H), 2.66 (t, *J* = 6.5 Hz, 2H), 2.15 (t, *J* = 6.4 Hz, 2H), 0.98–1.20 (m, 4H); ¹³C NMR (75 MHz, D₂O) δ 178.0, 153.8, 133.4, 127.2, 115.1, 45.6, 42.8, 31.9, 28.1; GC–MS *m/z* 209 (MH)⁺.

4-[[[(Benzyloxy)carbonyl](4-[[[(benzyloxy)carbonyl]-amino]butyl)amino]benzoic Acid (12)

Benzyl chloroformate (5.2 g, 0.31 mol) was added dropwise at 0 °C to a solution of **11** (4.84 g, 0.022 mol) in sodium phosphate buffer (pH 12, 176 mL). The reaction proceeded at room temperature for 24 h, yielding a mixture of benzyloxycarbonyl (Cbz) adducts. The mixture was acidified with HCl and extracted with CH₂Cl₂ (3 × 25 mL), and the extracts were evaporated under reduced pressure. The resulting crystalline material was stirred in 1 M KOH (44 mL) and dioxane (100 mL) until a single product was detected with TLC. The solution was acidified with HCl to pH < 1, extracted with CH₂Cl₂ (3 × 25 mL), dried (Na₂SO₄), and evaporated under reduced pressure. The resulting oil was purified on a silica gel column; elution with

hexane/EtOAc (1:1) gave **12** as a white crystalline solid (7 g, 68% yield). ¹H NMR (300 MHz, CDCl₃) δ 7.79 (d, *J* = 9 Hz, 2H), 7.25 (m, 12H), 6.50 (s, 1H), 5.13 (s, 2H), 5.05 (s, 2H), 3.70 (br t, 2H), 3.10 (br q, 2H), 1.55 (m, 4H); ¹³C NMR (75 MHz, CDCl₃) δ 169.0, 156.4, 155.0, 144.8, 136.5, 136.2, 131.3, 128.3, 128.0, 127.7, 126.7, 67.5, 66.5, 49.6, 41.0, 26.9, 25.5.

2-(Dimethylamino)ethyl 4-[[[(Benzyloxy)carbonyl](4-[[[(benzyloxy)carbonyl]amino]butyl]amino]benzoate (**13**)

N,N'-Carbonyldiimidazole (1.18 g, 7 mmol) was added to a solution of **12** (3.1 g, 6.6 mmol) in dry glyme (40 mL) under N₂. The reaction was heated to just below boiling for 2 h, followed by the addition of 2-(dimethylamino)ethanol (1.77 g, 0.02 mol) and NaH (~2 mg). After 8 h the reaction was complete as judged by TLC. The solvent was removed in vacuo and the resulting residue was dissolved in CCl₄ (50 mL). After extraction with H₂O (3 × 30 mL), the organic phase was dried over Na₂SO₄ and the solvent was evaporated under reduced pressure. The resulting oil was purified on a silica gel column eluted with EtOAc/IPA (9:1), yielding pure **13** as a yellowish gum (3.3 g, 92% yield). ¹H NMR (300 MHz, CDCl₃) δ 8.05 (d, *J* = 9 Hz, 2H), 7.31 (m, 12H), 5.15 (s, 2H), 5.07 (s, 2H), 4.78 (s, 1H), 4.45 (t, *J* = 6.7 Hz, 2H), 3.73 (t, *J* = 6.6 Hz, 2H), 3.15 (br q, 2H), 2.74 (t, *J* = 6.5 Hz, 2H), 2.33 (s, 6H), 1.56 (m, 4H); ¹³C NMR (75 MHz, CDCl₃) δ 165.8, 156.2, 154.2, 145.8, 136.5, 136.2, 130.4, 128.4, 128.0, 127.7, 126.4, 67.4, 66.5, 63.0, 57.7, 49.6, 45.7, 40.5, 27.0, 25.5.

2-(Dimethylamino)ethyl 4-[(4-Aminobutyl)amino]benzoate (**14**)

Pd/C (0.2 g, 10%) was added to a solution of **13** (3.2 g, 5.9 mmol) in concentrated acetic acid (8 mL). The resulting suspension was stirred rapidly under 1 atm of H₂ until the uptake of H₂ ceased. The reaction mixture was filtered and the filtrate was evaporated to yield 2 g (99% yield) of **14** as pale yellow crystals. ¹H NMR (500 MHz, CD₃OD) δ 7.81 (d, *J* = 9 Hz, 2H), 6.61 (d, *J* = 9 Hz, 2H), 5.15 (br s, 3H, *NH*), 4.48 (t, *J* = 5 Hz, 2H), 3.17–3.22 (m, 4H), 2.96 (t, *J* = 8 Hz, 2H), 2.68 (s, 6H), 1.68–1.80 (m, 4H) (peak assignments were aided by ¹H–¹H COSY experiment); ¹³C NMR (125 MHz, CD₃OD) δ 168.2, 154.9, 132.9, 117.3, 112.3, 61.0, 57.9, 44.7, 43.4, 40.5, 27.1, 26.4; MS (ESI) *m/z* 280.1 (MH)⁺.

2-(Dimethylamino)ethyl 4-[[4-(Acetylamino)butyl]-amino]benzoate (**15**)

A mixture of **14** (0.279 g, 1 mmol) and acetic acid *N*-hydroxysuccinimide ester (0.157 g, 1 mmol) in 10 mL of ethanol was stirred at room temperature for 4 h. Reaction progress was followed by TLC. Removal of solvent in vacuo gave a residue that was purified on a silica gel column; elution with 2-propanol/MeOH (1:1) gave 161 mg (50%) of **15**. ¹H NMR (400 MHz, CD₃OD) δ 7.81 (d, *J* = 9 Hz, 2H), 6.59 (d, *J* = 9 Hz, 2H), 5.21 (br s, 1H, *NH*), 4.55 (t, *J* = 5 Hz, 2H), 3.43 (br s, 2H), 3.19 (t, *J* = 7 Hz, 2H), 3.15 (t, *J* = 7 Hz, 2H), 2.87 (s, 6H), 1.93 (s, 3H), 1.55–1.66 (m, 4H) (peak assignments were aided by ¹H–¹H COSY experiment); ¹³C NMR (125 MHz, CD₃OD) δ 173.3, 168.0, 155.0, 133.0, 116.8, 112.2, 59.9, 57.5, 44.0, 43.6, 40.3, 28.0, 27.5, 22.8; MS (ESI) *m/z* 322.2 (MH)⁺.

4-Aminobenzoic Acid 2-(Dimethylamino)ethyl Ester (**16**)

A mixture of *p*-nitrobenzoyl chloride (30 g, 0.162 mol) and 2-(dimethylamino)ethanol (43.2 g, 0.486 mol) in 500 mL of dry benzene was stirred at room temperature for 14 h to form 4-nitrobenzoic acid 2-(dimethylamino)ethyl ester. Following acidification with cold dilute HCl, the aqueous phase was extracted with ether and made alkaline with sodium carbonate. The oil that separated was extracted twice with ether, and the extracts were washed with water and dried over potassium carbonate. 4-Nitrobenzoic acid 2-(dimethylamino)-ethyl ester was precipitated with the addition of dry HCl and recrystallized from absolute ethanol (32.8 g, 85% yield). 4-Nitrobenzoic acid 2-(dimethylamino)ethyl ester (15 g, 63 mmol) in absolute EtOH (125 mL) was added to SnCl₂ (59.7 g, 315 mmol) and the mixture was stirred at 70 °C for 2.5

h. The reaction was cooled to room temperature and poured into 200 mL of ice/H₂O; saturated NaOH (420 mL) was added, followed by extraction with EtOAc and concentration in vacuo. The resulting residue was purified on a silica gel column. Elution with 2-propanol/MeOH (1:1) gave pure **16** (9.1 g, 70%). ¹H NMR (500 MHz, CD₃OD) δ 7.77 (d, *J* = 9 Hz, 2H), 6.63 (d, *J* = 9 Hz, 2H), 4.85 (s, 2H, NH), 4.35 (t, *J* = 5.5 Hz, 2H), 2.74 (t, *J* = 5.5 Hz, 2H), 2.34 (s, 6H); ¹³C NMR (125 MHz, CD₃OD) δ 168.7, 155.0, 132.8, 118.6, 114.4, 62.9, 58.9, 45.9; MS (ESI) *m/z* 209.0 (MH)⁺.

Acknowledgements

This work was supported by grants from the National Eye Institute (EY009275 to J.W.K. and EY012837 to R.L.B). We thank the Bioanalytical Shared Resource at OHSU for mass spectrometry data.

References

1. Fesenko EE, Kolesnikov SS, Lyubarsky AL. Induction by cyclic GMP of cationic conductance in plasma membrane of retinal rod outer segment. *Nature* 1985;313:310–313. [PubMed: 2578616]
2. Nakamura T, Gold GH. A cyclic nucleotide-gated conductance in olfactory receptor cilia. *Nature* 1987;325:442–444. [PubMed: 3027574]
3. Karpen JW, Zimmerman AL, Stryer L, Baylor DA. Gating kinetics of the cyclic-GMP-activated channel of retinal rods: flash photolysis and voltage-jump studies. *Proc Natl Acad Sci U S A* 1988;85:1287–1291. [PubMed: 2448798]
4. Heginbotham L, Abramson T, MacKinnon R. A functional connection between the pores of distantly related ion channels as revealed by mutant K⁺ channels. *Science* 1992;258:1152–1155. [PubMed: 1279807]
5. Doyle DA, Morais Cabral J, Pfuetzner RA, Kuo A, Gulbis JM, et al. The structure of the potassium channel: molecular basis of K⁺ conduction and selectivity. *Science* 1998;280:69–77. [PubMed: 9525859]
6. Jiang Y, Lee A, Chen J, Ruta V, Cadene M, et al. X-ray structure of a voltage-dependent K⁺ channel. *Nature* 2003;423:33–41. [PubMed: 12721618]
7. Henn DK, Baumann A, Kaupp UB. Probing the transmembrane topology of cyclic nucleotide-gated ion channels with a gene fusion approach. *Proc Natl Acad Sci U S A* 1995;92:7425–7429. [PubMed: 7543681]
8. Liu DT, Tibbs GR, Siegelbaum SA. Subunit stoichiometry of cyclic nucleotide-gated channels and effects of subunit order on channel function. *Neuron* 1996;16:983–990. [PubMed: 8630256]
9. Varnum MD, Zagotta WN. Subunit interactions in the activation of cyclic nucleotide-gated ion channels. *Biophys J* 1996;70:2667–2679. [PubMed: 8744304]
10. Becchetti A, Gamel K, Torre V. Cyclic nucleotide-gated channels. Pore topology studied through the accessibility of reporter cysteines. *J Gen Physiol* 1999;114:377–392. [PubMed: 10469728]
11. Flynn GE, Zagotta WN. Conformational changes in S6 coupled to the opening of cyclic nucleotide-gated channels. *Neuron* 2001;30:689–698. [PubMed: 11430803]
12. Zimmerman AL, Baylor DA. Cyclic GMP-sensitive conductance of retinal rods consists of aqueous pores. *Nature* 1986;321:70–72. [PubMed: 2422559]
13. Haynes LW, Kay AR, Yau KW. Single cyclic GMP-activated channel activity in excised patches of rod outer segment membrane. *Nature* 1986;321:66–70. [PubMed: 2422558]
14. Ruiz M, Karpen JW. Single cyclic nucleotide-gated channels locked in different ligand-bound states. *Nature* 1997;389:389–392. [PubMed: 9311781]
15. Kaupp UB, Seifert R. Cyclic nucleotide-gated ion channels. *Physiol Rev* 2002;82:769–824. [PubMed: 12087135]
16. Haynes LW. Block of the cyclic GMP-gated channel of vertebrate rod and cone photoreceptors by *l*-cis-diltiazem. *J Gen Physiol* 1992;100:783–801. [PubMed: 1282145]
17. Fodor AA, Gordon SE, Zagotta WN. Mechanism of tetracaine block of cyclic nucleotide-gated channels. *J Gen Physiol* 1997;109:3–14. [PubMed: 8997661]

18. Sunami A, Dudley SC Jr, Fozzard HA. Sodium channel selectivity filter regulates antiarrhythmic drug binding. *Proc Natl Acad Sci U S A* 1997;94:14126–14131. [PubMed: 9391164]
19. Ragsdale DS, McPhee JC, Scheuer T, Catterall WA. Molecular determinants of state-dependent block of Na⁺ channels by local anesthetics. *Science* 1994;265:1724–1728. [PubMed: 8085162]
20. Ragsdale DS, McPhee JC, Scheuer T, Catterall WA. Common molecular determinants of local anesthetic, antiarrhythmic, and anticonvulsant block of voltage-gated Na⁺ channels. *Proc Natl Acad Sci U S A* 1996;93:9270–9275. [PubMed: 8799190]
21. Catterall WA. Molecular mechanisms of gating and drug block of sodium channels. *Novartis Found Symp* 2002;241:206–218. [PubMed: 11771647]
22. Fodor AA, Black KD, Zagotta WN. Tetracaine reports a conformational change in the pore of cyclic nucleotide-gated channels. *J Gen Physiol* 1997;110:591–600. [PubMed: 9348330]
23. Ghatpande AS, Uma R, Karpen JW. A multiply charged tetracaine derivative blocks cyclic nucleotide-gated channels at subnanomolar concentrations. *Biochemistry* 2003;42:265–270. [PubMed: 12525153]
24. Root MJ, MacKinnon R. Identification of an external divalent cation-binding site in the pore of a cGMP-activated channel. *Neuron* 1993;11:459–466. [PubMed: 7691102]
25. Eismann E, Muller F, Heinemann SH, Kaupp UB. A single negative charge within the pore region of a cGMP-gated channel controls rectification, Ca²⁺ blockage, and ionic selectivity. *Proc Natl Acad Sci U S A* 1994;91:1109–1113. [PubMed: 7508120]
26. Zheng J, Trudeau MC, Zagotta WN. Rod cyclic nucleotide-gated channels have a stoichiometry of three CNGB1 subunits and one CNGB1 subunit. *Neuron* 2002;36:891–896. [PubMed: 12467592]
27. Zhong H, Molday LL, Molday RS, Yau KW. The heteromeric cyclic nucleotide-gated channel adopts a 3A:1B stoichiometry. *Nature* 2002;420:193–198. [PubMed: 12432397]
28. Weitz D, Ficek N, Kremmer E, Bauer PJ, Kaupp UB. Subunit stoichiometry of the CNG channel of rod photoreceptors. *Neuron* 2002;36:881–889. [PubMed: 12467591]
29. Heinemann SH, Terlau H, Stuhmer W, Imoto K, Numa S. Calcium channel characteristics conferred on the sodium channel by single mutations. *Nature* 1992;356:441–443. [PubMed: 1313551]
30. Zimmerman AL, Karpen JW, Baylor DA. Hindered diffusion in excised membrane patches from retinal rod outer segments. *Biophys J* 1988;54:351–355. [PubMed: 3207830]
31. Woodhull AM. Ionic blockage of sodium channels in nerve. *J Gen Physiol* 1973;61:687–708. [PubMed: 4541078]
32. Lu Z, Ding L. Blockade of a retinal cGMP-gated channel by polyamines. *J Gen Physiol* 1999;113:35–43. [PubMed: 9874686]
33. Kramer RH, Karpen JW. Spanning binding sites on allosteric proteins with polymer-linked ligand dimers. *Nature* 1998;395:710–713. [PubMed: 9790193]

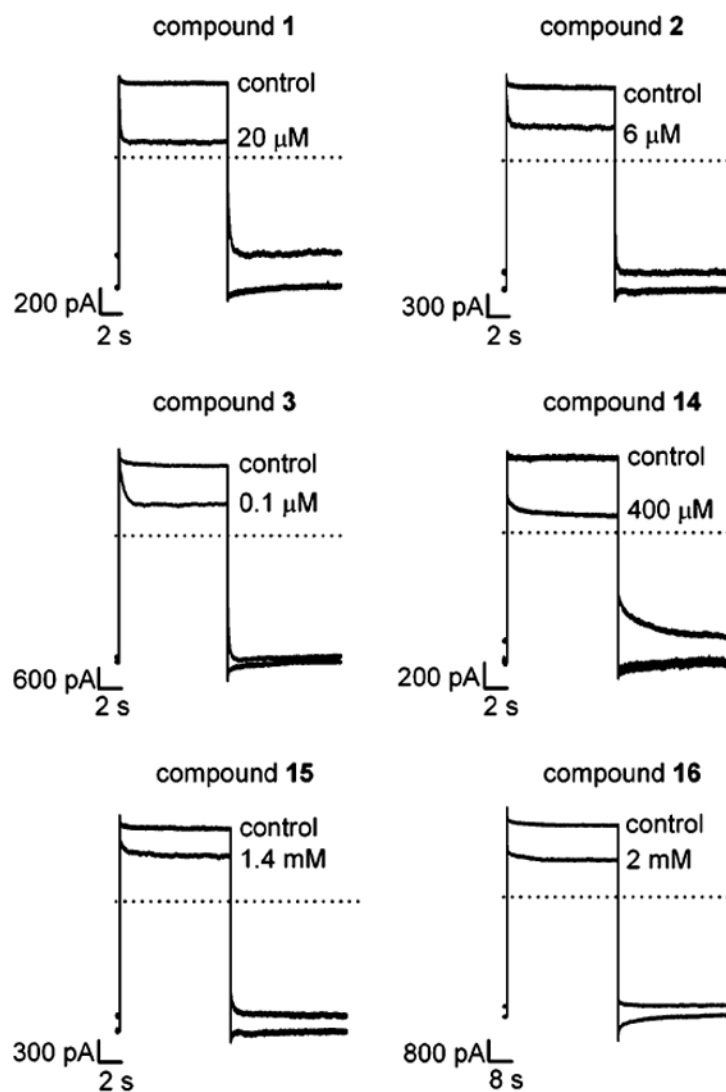


Figure 1. Representative current traces for CNGA1 channels under control conditions and with the indicated concentration of tetracaine analogue. The membrane potential was stepped from -80 to +40 and back to -80 mV. Each analogue is identified above the traces, and the dotted line represents the zero current level.

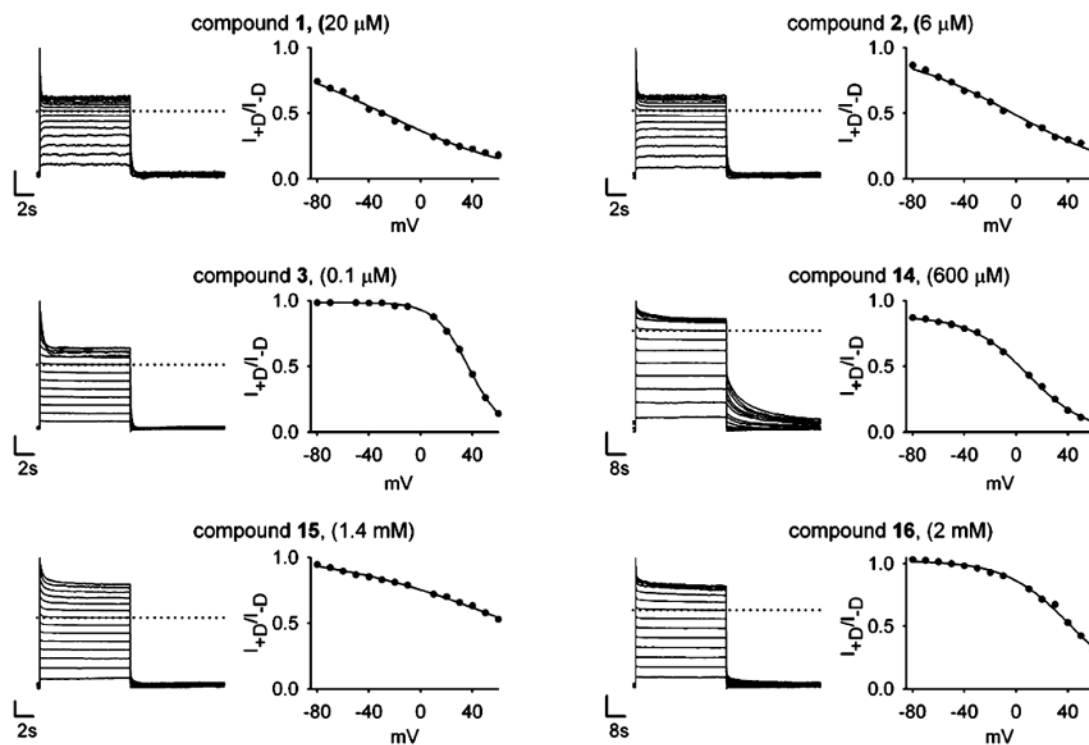
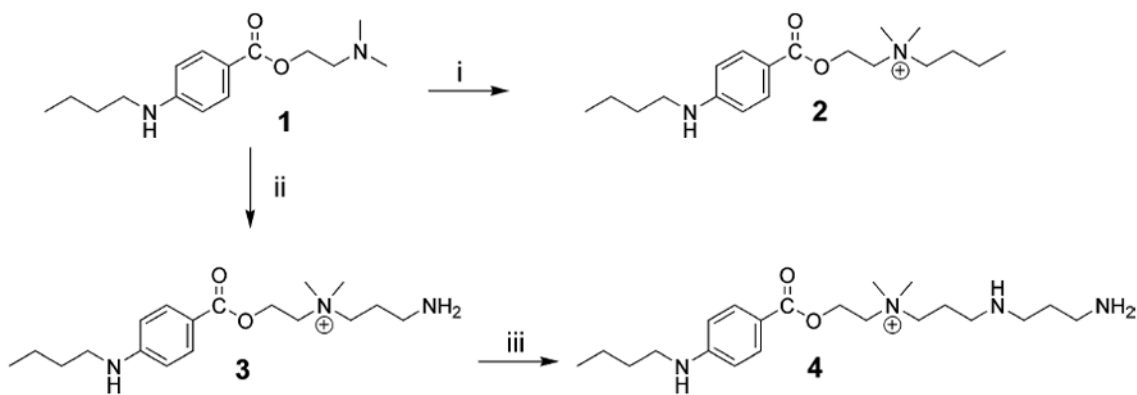
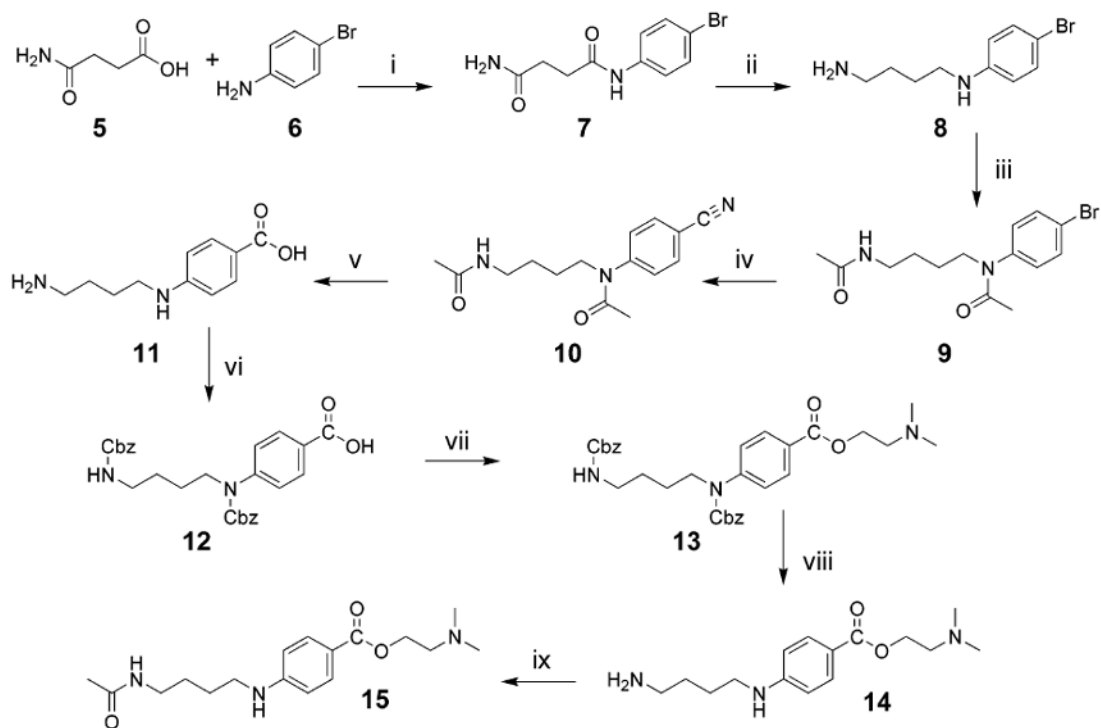


Figure 2.

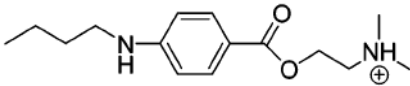
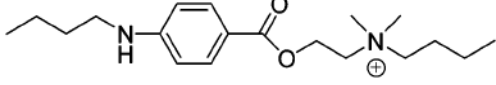
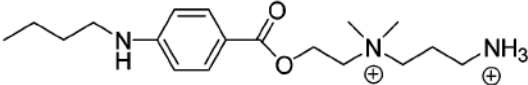
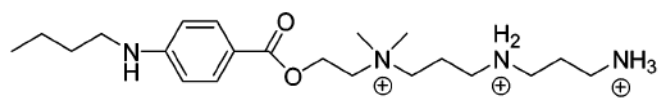
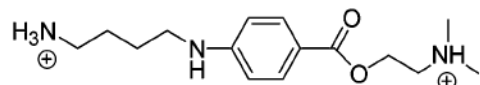
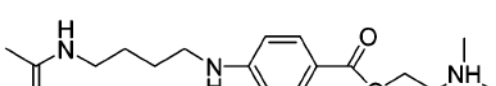
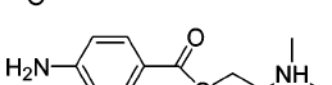
Voltage dependence of block. Representative current traces are shown for a series of depolarizations from -80 to +60 mV in 10 mV increments with each analogue. The vertical scale bar represents 1 nA. Compounds and concentrations employed are indicated. The fraction of current remaining relative to control at each potential is plotted alongside. The data are fit with the Woodhull model for voltage-dependent block (Table 1). The apparent dissociation constant at 0 mV, $K_{D(0)}$, and the effective valence, $z\delta$, of each blocker from several patches are displayed in Table 1. The zero current level is indicated by the dotted line.

**Scheme 1.**Derivatization of the Tertiary Amine of Tetracaine^a^aReagents/conditions: (i) 1-bromobutane in EtOH/ Δ ; (ii) 3-bromopropylamine in EtOH/ Δ ; (iii) 3-bromopropylamine in EtOH/ Δ .

**Scheme 2.**Analogues of Tetracaine with Modifications at the Butyl Tail^a

^aReagents/conditions: (i) carbonyldiimidazole in DMF; (ii) borane dimethyl sulfide in THF/ Δ , HCl; (iii) acetic anhydride and triethylamine in CH_2Cl_2 , NaOH; (iv) CuCN in NMP/ Δ ; (v) HBr/ Δ ; (vi) benzyl chloroformate (CbzCl) in phosphate buffer, KOH; (vii) carbonyldiimidazole in glyme/ Δ , 2-(dimethylamino)ethanol and NaH/ Δ ; (viii) H_2 /Pd in acetic acid; (ix) acetic acid NHS ester in EtOH.

Table 1
Tetracaine Analogue Structures and Block of CNGA1 Channels

compound ^a		$K_{D(40)}$ (μM) ^b	$K_{D(40)}$ (μM) ^c	$z\delta$ ^c
1d		6.8 ± 7.7 (21) ^e	12 ± 5 (7)	0.47 ± 0.03
2		3.1 ± 0.7 (5)	5.4 ± 1.6 (5)	0.45 ± 0.04
3		0.074 ± 0.037 (8)	10.4 ± 0.7 (5)	1.8 ± 0.2
4f		$3.0 \times 10^{-5} \pm 2.0 \times 10^{-5}$ (7)	0.0069 ± 0.0047 (5)	2.6 ± 0.3
14		210 ± 110 (18)	970 ± 390 (9)	1.1 ± 0.1
15		2500 ± 800 (11)	4000 ± 800 (4)	0.47 ± 0.09
16		2300 ± 1300 (14)	10000 ± 5700 (5)	0.91 ± 0.17

^aThe compounds are depicted here in what is expected to be the predominant protonation state at pH 7.6.

^b $K_{D(40)}$ is the apparent dissociation constant at +40 mV, calculated from the equation $I_{+D}/I_{-D} = K_{D(40)}/\{K_{D(40)} + [D]\}$, where the left side is current in the presence of blocker divided by current in the absence of blocker, and [D] is blocker concentration.

^c $K_{D(0)}$, the apparent dissociation constant at 0 mV, and $z\delta$, the effective valence of the blocker, were determined from fits (Figure 2) of the Woodhull equation:³² $I_{+D}/I_{-D} = K_{D(0)}e^{(-z\delta FV/RT)}/\{K_{D(0)}e^{(-z\delta FV/RT)} + [D]\}$.

^dThe $K_{D(40)}$ reported previously²³ was significantly lower, due to the use of a lower pH solution in those experiments.

^eThe number of patches tested is indicated in parentheses. For all of the compounds tested here, the patch to patch variability in the efficiency of block was quite high. The reasons for this are unknown.

^fTo prevent breakdown over time, compound **4** must be stored desiccated at -80°C .